Design of multi-resonance thermally activated delayed fluorescence materials for organic light-emitting diodes

Jingxiang Wang*, Tomas Matulaitis* Sudhakar Pagidi*, Eli Zysman-Colman*

*** Organic Semiconductor Centre, EaStCHEM School of Chemistry, University of St Andrews, St Andrews, UK, KY16 9ST. E-mail: eli.zysman-colman@st-andrews.ac.uk**

Abstract

Two strategies to improve the performance of multiresonant thermally activated delayed fluorescence (MR-TADF) compounds are explored. These include incorporation of units to turn on aggregation-induced emission so as to permit use of MR-TADF compounds at high doping concentrations, and the use of heavy atoms to increase spin-orbit coupling to enhance reverse intersystem crossing rates. Preliminary photophysical investigations are presented.

Author Keywords

Fluorescence; aggregation-induced emission; heavy atom effect; multi-resonant thermally activated delayed fluorescence.

1. Introduction

Organic light-emitting diodes (OLEDs) are a disruptive technology for displays, fast overtaking market share from liquid crystalline displays (LCDs). OLEDs have many advantages in terms of performance such as their high dynamic color range, fast refresh rates, light and ultrathin profiles and low power consumption. Commercial vacuum-deposited OLEDs employ fluorescent blue emitters and phosphorescent green and red emitters. Much recent excitement has focused on the development of purely organic thermally activated delayed fluorescence (TADF) emitters as these compounds can achieve comparable internal quantum efficiencies without the use of scarce and expensive noble metals. In typical OLEDs, the emitter is doped at low concentration into a host matrix in part to mitigate against aggregation-caused quenching. Further, most TADF OLEDs show severe efficiency roll-off at high luminance, this in part due to the too high triplet exciton density linked to inefficient TADF associated with too slow a reverse intersystem crossing rate constant, k_{RISC}. Developing solutions to address these two issues are necessary to overcome the barriers to commercial adoption of these materials within the OLED industry.[1]

In 2001, Tang and co-workers coined the term aggregation-induced emission (AIE) to describe an enhancement of the photoluminescence quantum yield (Φ_{PL}) at elevated concentrations of emitter.[2] The compound in their seminal study, 1-methyl-2,3,4,5 pentaphenylsilole (MPPS), is virtually non-emissive in dilute solution; however, shows bright fluorescence in the aggregated state. Emission enhancement was attributable to the restriction of molecular motions in the aggregated state. Since then, numerous AIE-active molecules have been designed and exploited in a number of applications, including bio-imaging, sensors, electroluminescent devices. AIE behavior can frequently be conferred upon a molecule through the incorporation of "AIEgens" such as cyclic siloles and tetraphenylethene (TPE). For instance, TPE and triphenylamine (TPA) have Φ_{PL} of 49.2% and 10.2%, respectively, in amorphous films but when the fragments are integrated into a single molecule the Φ_{PL} increases to 92% and 100%, respectively, in tris(4'-(1,2,2-triphenylvinyl)-[1,1'-biphenyl]-4-yl)amine (3TPETPA) and $N^4,N^4,N^{4'},N^{4'}$-tetrakis(4'-(1,2,2-triphenylvinyl)-[1,1'-biphenyl]-4-yl)-[1,1'-biphenyl]-4,4' diamine (4TPEDTPA).[3] These two examples demonstrate how non-radiative decay pathways in the aggregated state are suppressed when TPE units are present.

There are now numerous TADF materials with AIE-activity, termed AIDF for aggregation-induced delayed fluorescence. These are excellent candidates for use in non-doped OLEDs. For instance, Tang and co-workers demonstrated non-doped yellow OLEDs (λ_{EL} = 548 nm) with an excellent maximum external quantum efficiency (EQE_{max}) of 22.6%, negligible efficiency roll-off (20.1% at 5000 cd m^{-2}) and improved operational stability with an emissive layer (EML) containing DCB-BP-PXZ (Figure 1).[4] This compound shows a Φ_{PL} in THF of only 4%, which increases to 69% in the neat film, showing a λ_{PL} of 530 nm, a short delayed fluorescence lifetime, τ_d, of 2.6 μs and a singlet-triplet energy gap, ΔE_{ST}, of 0.024 eV. Despite the wide use of TPE in AIE-active compounds, to the best of our knowledge there is only a single example of a TPE-containing AIDF emitter. The compound ECDPTT was used in the EML of a non-doped green OLED (λ_{EL} = 517 nm), which exhibited a maximum current efficiency and a maximum luminance of 2.478 cd A^{-1} and 7561 cd m^{-2}, respectively.[5] The material emits at 558 nm in the neat film and has a small ΔE_{ST} of 0.12 eV and a τ_d of 2.12 μs. Zhao *et al.* designed an AIDF emitter, 4,4-CzSPz, showing a high Φ_{PL} of 97% with an emission centered at 530 nm in the neat film.[6] This compound posseses a τ_d of 62.2 μs despite the small ΔE_{ST} of 0.024 eV. The non-doped device showed an EQE_{max} of 20% at a λ_{EL} of 526 nm. A solution-processed sky-blue non-doped AIDF OLED was reported by Wu *et al*. using m-ACSO2 as the emitter that showed an EQE_{max} of 17.2% at a λ_{EL} of 486 nm.[7] Additionally, efficiency roll-off was low with an EQE at 100 cd m^{-2} of 16.5%. This material emits at 473 nm, and has a Φ_{PL} of 76%, a τ_d of 3.2 μs and a ΔE_{ST} is 0.07 eV in the neat film. Recently, Leng *et al.* reported the AIDF compound mPhDCzDPSPXZ that emits at 548 nm and has a Φ_{PL} of 56%, a short τ_d of 0.76 μs and a ΔE_{ST} is 0.03 eV in the neat film.[8] Non-doped devices showed EQE_{max} of 18.1% at a λ_{EL} of 523 nm; the efficiency roll-off was low with an EQE at 1000 cd m^{-2} of 16.9%. These exemplar studies clearly illustrate the potential of AIDF materials for use as emitters in non-doped OLEDs as these devices tend to offer excellent efficiencies and extremely small efficiency roll-off.

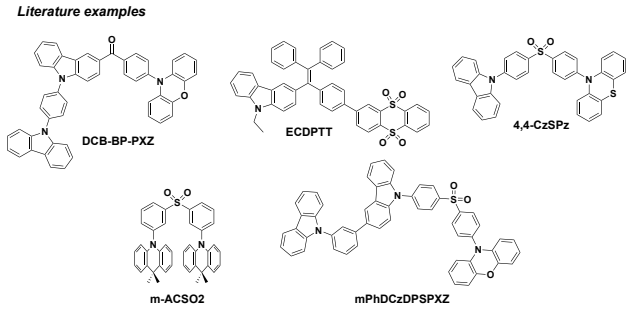

Figure 1. Chemical structure of literature examples of AIDF compounds.

The magnitude of the first order mixing coefficient, λ, between the S_1 and T_1 states provides a useful tool to assess the efficiency of TADF. The parameter λ is proportional to the square of the spin-orbital coupling (SOC) matrix element and inversely proportional to ΔE_{ST}. Thus, the efficiency of TADF can be improved by reducing ΔE_{ST}, which is a guiding principle of TADF emitter design, and by enhancing SOC. SOC itself scales with Z^4, where Z is the atomic number of the atoms involved in the transitions to the S_1 and T_1 states, which is the origin of the so-called heavy atom effect.[9] The incorporation of heavy atoms such as bromine, sulfur or selenium has been used as an effective strategy in donor-acceptor TADF emitter design to increase k_{RISC}.[10-17]

Multi-resonant (MR-TADF) molecules are a sub-class of TADF emitters that are based on n- and p- doped nanographene that contain atoms such as boron and nitrogen. A small exchange integral and therefore a small ΔE_{ST} is maintained as a result of the opposing resonance effect of these atoms. The spectroscopic signature of this class of compounds is one of a very narrow emission due to their rigid nature that shows a small degree of positive solvatochromism as a result of the short-range charge transfer nature of the lowest excited states (S_1 and T_1).[18] Unfortunately, most MR-TADF emitters show moderately large ΔE_{ST} (ca. 150-200 meV) and this leads to relatively slow k_{RISC} and thus severe efficiency roll-off in the OLEDs. One strategy to overcome this design weakness would be to include heavy atoms into the design of MR-TADF emitters.[19] Further, MR-TADF compounds are typically planar and thus tend to aggregate easily, resulting in severe aggregation-caused quenching at even moderate doping concentrations within the emissive layer. Incorporation of AIEgens may be a route to overcoming this design weakness. Here, we present two triangulene compounds, **dBr-tBu-DiKTa** and **TPE-tBu-DiKTa**, designed to increase k_{RISC} and be used at high doping, respectively, and report an initial photophysical assessment.

2. Computational Modelling

The electronic structures of **dBr-tBu-DiKTa** and **TPE-tBu-DiKTa** were modelled using Density Functional Theory at the PBE0/6-31G(d,p) level of theory in the gas phase (Figure 2). The Highest Occupied Molecular Orbital (HOMO) is distributed over the entire compound, save for the ^{t}Bu group, while the Lowest Unoccupied Molecular Orbital (LUMO) is localized mainly on the central triangulene fragment. The pattern of the electron density distribution about the triangulene core is reminiscent of the parent **DiKTa** emitter.[18] The small redistribution in the electron density distribution is reflected in the small permanent and transition dipoles of 2.71 and 4.24 D, and 6.68 and 4.33 D, respectively, for **dBr-tBu-DiKTa** and **TPE-tBu-DiKTa**. The calculated energies of the S_1 state are 3.24 and 2.86 eV, respectively, for **dBr-tBu-DiKTa** and **TPE-tBu-DiKTa**, this state is characterized mainly by a HOMO-LUMO transition that shows the signature of a MR-TADF emitter. The energies of the T_1 state are 2.55 and 2.38 eV, respectively, for **dBr-tBu-DiKTa** and **TPE-tBu-DiKTa**. The additional conjugation arising from the TPE group results in a stabilization of both these states in the latter compound. There are additionally two intermediate triplet states at 3.07 and 3.14 eV for **dBr-tBu-DiKTa** and 2.49 and 2.52 eV for **TPE-tBu-DiKTa**. Spin-vibronic coupling from T_1 to these states is likely to assist the TADF process. The calculated ΔE_{ST} value of 0.69 eV for both compounds determined by TDA-DFT are expectedly overestimated, SCS-CC2 calculations would be required to accurately predict this value, calculations that are ongoing.[20]

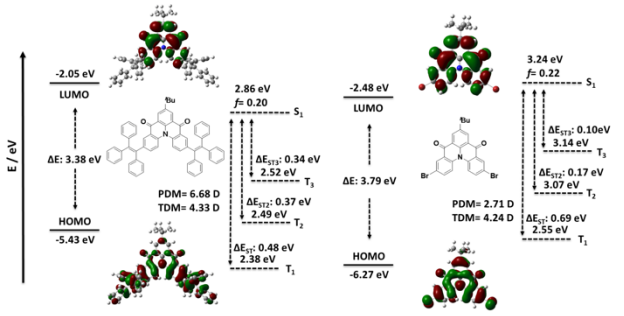

Figure 2. HOMO and LUMO electron density distributions and energy levels (in eV), excited state energy levels (in eV) of (left) **TPE-tBu-DiKTa** and (right) **dBr-tBu-DiKTa**.

3. Synthesis

TPE-tBu-DiKTa was obtained following a six-step linear sequence as outlined in Figure 3. Intermediate **1** was obtained via a high-temperature double Ullman coupling between 4-*tert*-butylaniline and methyl 2-iodobenzoate in 67% yield. Regioselective bromination afforded compound **2** in 67% yield.[21] Saponification to generate quantitatively intermediate **3** followed by activation of the diacid with thionyl chloride and cyclization in the presence of $AlCl_3$ afforded **dBr-*t*Bu-DiKTa**, in 73% yield. Palladium-catalyzed borylation installed the diboronate ester groups in **4** in 75% yield, which was then reacted with the vinyl bromide under Suzuki-Miyaura cross-coupling conditions to furnish **TPE-tBu-DiKTa** in 54% yield.

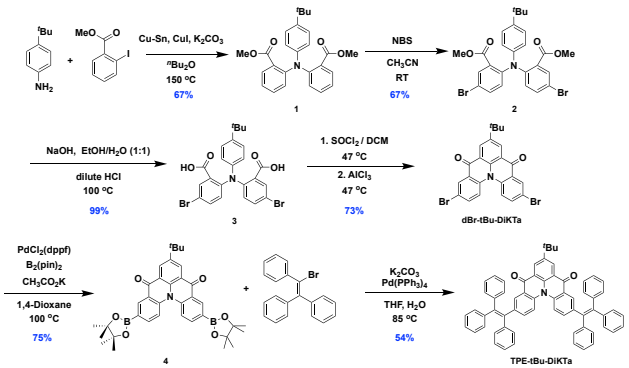

Figure 3. Synthesis scheme of **TPE-tBu-DiKTa**.

4. Optoelectronic Characterization

Figure 4(a) shows the cyclic and differential pulse voltammograms in DCM, referenced versus SCE, of **dBr-tBu-DiKTa** and **TPE-tBu-DiKTa**. Both compounds show reversible reduction waves at -1.50 and -1.58 V, respectively, and mostly irreversible oxidation waves at 1.56 and 1.13 V, respectively. The corresponding HOMO/LUMO values for **dBr-tBu-DiKTa** and **TPE-tBu-DiKTa** are, respectively, -5.90/-2.84 eV and -5.47/-2.76 eV. The trends in the electrochemical data match those predicted by DFT calculations. The HOMO value for **dBr-tBu-DiKTa** is similar to that of the parent compound **DiKTa** (-5.93 eV) while the LUMO value is cathodically shifted compared to **DiKTa** (-3.11 eV).[18] The profiles of the UV-visible absorption spectra of the two compounds in toluene are similar with low energy bands (molar absorptivities, ε, at 424 (11×10^3 M^{-1} cm^{-1}) and 445 nm (30×10^3 M^{-1} cm^{-1}) for **dBr-tBu-DiKTa** and 439 (12×10^3 M^{-1} cm^{-1}) and 461 nm (23×10^3 M^{-1} cm^{-1}) for **TPE-tBu-DiKTa** (Figure 4b). The similar ε values for the low-energy short-range charge transfer (SRCT) band are reflected in the similar TDA-DFT calculated oscillator strengths for to the $S_0\rightarrow S_1$ transition (Figure 2). The absorption spectrum of **dBr-tBu-DiKTa** matches well that of the parent compound **DiKTa** while the highly absorptive band at 346 nm (ε = 39×10^3 M^{-1} cm^{-1}) in **TPE-tBu-DiKTa** is associated with a locally excited transition on the TPE moiety.

Both compounds show a small degree of positive solvatochromism that is characteristic of a SRCT excited state associated with MR-TADF compounds. The photoluminescence maxima (full-width at half maximum), λ_{PL}, in toluene for **dBr-tBu-DiKTa** and **TPE-tBu-DiKTa** are 466 nm (25 nm) and 490 nm (40 nm), respectively (Figure 4b); the emission maximum for **dBr-tBu-DiKTa** aligns well with that previously reported for this compound in DCM[22] and is slightly red-shifted compared to **DiKTa** (λ_{PL} = 453 nm). The presence of the TPE groups result in a stabilization of the emissive S_1 state, as predicted by TDA-DFT calculations, and a turn-on of the AIE behavior (Figure 4c). Indeed, there is a progressive red-shifting of the λ_{PL} with increasing water content in THF:H_2O mixtures up to 50%, this associated with a decrease in emission intensity. There is then a change in behavior for 50-70% water fraction in THF that is associated with a blue-shift in λ_{PL} and a dramatic enhancement in emission intensity. The emission intensity modestly decreases from 70-90% water fraction in THF while the λ_{PL} remains largely unchanged. To the best of our knowledge, this is the first demonstration of AIE in a MR-TADF emitter. By contrast, there is no emission enhancement and a modest blue-shift of the emission maximum for **dBr-tBu-DiKTa** with an increase in water content, which means this compound does not show AIE.

For **dBr-tBu-DiKTa**, the 77 K prompt fluorescence spectrum (λ_{PL} = 470 nm) in 2-MeTHF glass overlaps with the room-temperature steady-state (SS) PL spectrum. This indicates there is essentially no change in conformation of the compound across this temperature range. The phosphorescence spectrum is red-shifted at 520 nm, leading to a ΔE_{ST} of 0.25 eV, measured from the onset of the prompt fluorescence and phosphorescence spectra, respectively (Figure 5c). The prompt fluorescence spectrum of **TPE-tBu-DiKTa** in 2MeTHF glass at 77 K is slightly blue-shifted (λ_{PL} = 499 nm) compared to the room-temperature SS PL spectrum (λ_{PL} = 504 nm). Surprisingly, we could not detect any phosphorescence in this compound in this medium.

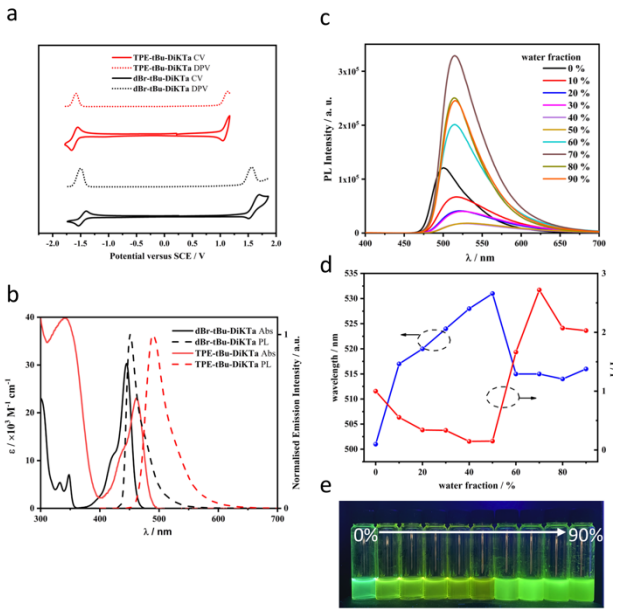

Figure 4. **a)**. CV and DPV in DCM with with 0.1 M [^{n}Bu$_4$N]PF$_6$ for **dBr-tBu-DiKTa** and **TPE-tBu-DiKTa**; **b)** absorption and photoluminescence spectra in toluene (λ_{exc} = 340 nm and 346 nm) for **dBr-tBu-DiKTa** and **TPE-tBu-DiKTa**; **c)** PL spectra as a function of water content in THF:H_2O mixture (λ_{exc} = 346 nm) for **TPE-tBu-DiKTa**; **d)** changes in λ_{PL} and PL intensity as a function of water fraction in THF: H_2O mixture; **e)**, Photos of solutions ranging from 100% THF to 90%H_2O/THF.

We then investigated the PL behavior of **dBr-tBu-DiKTa** in the solid state as doped thin films in mCP as the host matrix. As can be noted in Figures 5a and b, like most of the reported MR-TADF emitters, **dBr-tBu-DiKTa** is prone to aggregate. Indeed, upon increasing the doping concentration from 1 to 10 wt%, a 13 nm red-shift and broadening (FWHM increases by 15 nm) of the PL is observed. In the 10 wt% doped thin films in mCP, the prompt fluorescence spectrum and phosphorescence spectra are red-shifted compared to those in the 77 K 2-MeTHF glass at 504 nm and 529 nm, respectively. The corresponding ΔE_{ST} of 0.18 eV, measured from the onset of the prompt fluorescence and phosphorescence spectra, respectively, is slightly smaller (Figure 5d). The Φ_{PL} under a N_2 atmosphere is 43%, which drops to 30% when measured under air. The Φ_{PL} increased to 71% at 1 wt% doping. By contrast, the Φ_{PL} for a 10 wt% doped film of **DiKTa** in mCP was 16%, which increased to 40% at 3.5 wt% doping; the corresponding vacuum-deposited film at 3.5 wt% doping showed a Φ_{PL} of 75%. The time-resolved PL of a 1 wt% doped film decays with multiexponential kinetics; a prompt fluorescence lifetime, τ_p, of 6.5 ns, while delayed fluorescence is dominated by a long-lived component. The average delayed emission lifetime, τ_d, is 267 µs. **DiKTa** shows a much shorter τ_d of 23 µs in a 3.5 wt% doped film. For **TPE-tBu-DiKTa** in 10 wt% mCP, the prompt fluorescence shows a λ_{PL} at 513 nm, which slightly blues-shifts to 507 nm at room-temperature. Again, we did not detect any phosphorescence at low temperature, while at room temperature the PL decays with monoexponential kinetics with a lifetime of 5.1 ns. The Φ_{PL} of a

1 wt% doped film in mCP under N_2 is 31.0%, which decreased to 23.1% as a 10 wt% doped film, decreasing further to 18.3 and 14.7% as 50% doped films and neat films, respectively. Thus, the AIE behavior observed in the THF:water mixtures is not reproduced in the thin film state, suggesting that the aggregate species responsible for the AIE are not formed during the spin-coating conditions used to fabricate the films.

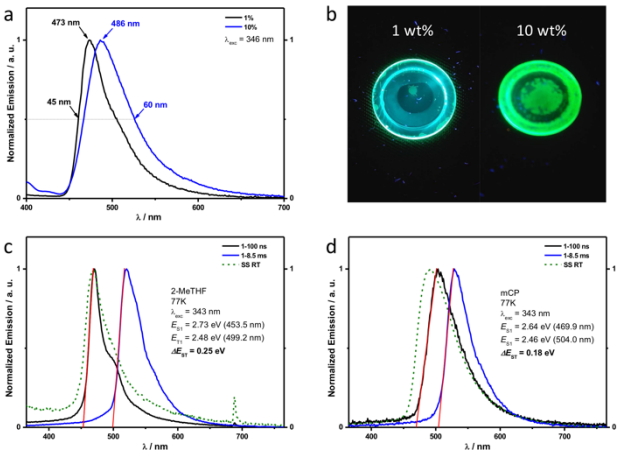

Figure 5. **a)**. Steady-state PL spectra of 1 and 10 wt% **dBr-tBu-DiKTa** doped films in mCP; **b)**. Photos of actual films illuminated by UV light (λ_{exc} = 365 nm); **c)**. Prompt fluorescence and phosphorescence spectra at 77 K in 2-MeTHF glass and stead-state PL spectrum at room temperature in 2-MeTHF (λ_{exc} = 343 nm) for **dBr-tBu-DiKTa**; **d).** Prompt fluorescence and phosphorescence spectra at 77 K in 10 wt% doped film in mCP and stead-state PL spectrum at room temperature in in 10 wt% doped film in mCP (λ_{exc} = 343 nm) for for **dBr-tBu-DiKTa**.

5. Outlook

We have briefly reviewed the state-of-the-art of AIE-TADF compounds and also TADF compounds bearing a heavy atom that can aid in both intersystem crossing and reverse intersystem crossing rates. We have reported preliminary photophysical characterization of a two triangulene compound derivatives of the previously reported MR-TADF emitter **DiKTa**. **TPE-tBu-DiKTa** does show AIE behavior and DFT calculations are promising; however, unexpectedly, we cannot detect any delayed fluorescence and the photoluminescence quantum yield of this compound is not sensitive to oxygen. Optoelectronic characterization of **dBr-tBu-DiKTa** reveals its potential, with a higher Φ_{PL}, a smaller ΔE_{ST} than the parent compound in mCP doped films. Current efforts are underway to fabricate OLEDs with the latter compound and to explore in more detail the photophysics of the former.

6. Acknowledgements

This project has received funding from the European Union's Horizon 2020 research and innovation programme under the Marie Skłodowska Curie grant agreement no. 891606 (TADFNIR). We are also grateful for financial support from the University of St Andrews Restarting Research Funding Scheme (SARRF), which is funded through the Scottish Funding Council grant reference SFC/AN/08/020. J.W. thanks the China Scholarship Council (202006250026). We thank the Engineering and Physical Sciences Research Council for support (EP/P010482/1, EP/R511778/1 and EP/L017008/1). We thank Umicore for the gift of palladium catalysts.

7. References

1. Liu H, Guo J, Zhao Z, Tang BZ. Aggregation-Induced Delayed Fluorescence. ChemPhotoChem. 2019;3(10):993-9.
2. Zhao Z, Zhang H, Lam JWY, Tang BZ. Aggregation-Induced Emission: New Vistas at the Aggregate Level. Angew Chem Int Ed. 2020;59(25):9888-907.
3. Yuan WZ, Lu P, Chen S, Lam JWY, Wang Z, Liu Y, et al. Changing the Behavior of Chromophores from Aggregation-Caused Quenching to Aggregation-Induced Emission: Development of Highly Efficient Light Emitters in the Solid State. Adv Mater. 2010;22(19):2159-63.
4. Liu H, Zeng J, Guo J, Nie H, Zhao Z, Tang BZ. High-Performance Non-doped OLEDs with Nearly 100 % Exciton Use and Negligible Efficiency Roll-Off. Angew Chem Int Ed. 2018;57(30):9290-4.
5. Dong X, Wang S, Gui C, Shi H, Cheng F, Tang BZ. Synthesis, aggregation-induced emission and thermally activated delayed fluorescence properties of two new compounds based on phenylethene, carbazole and 9,9′,10,10′-tetraoxidethianthrene. Tetrahedron. 2018;74(4):497-505.
6. Zhao J, Chen X, Yang Z, Liu T, Yang Z, Zhang Y, et al. Highly-Efficient Doped and Nondoped Organic Light-Emitting Diodes with External Quantum Efficiencies over 20% from a Multifunctional Green Thermally Activated Delayed Fluorescence Emitter. J Phys Chem C. 2019;123(2):1015-20.
7. Wu K, Wang Z, Zhan L, Zhong C, Gong S, Xie G, et al. Realizing Highly Efficient Solution-Processed Homojunction-Like Sky-Blue OLEDs by Using Thermally Activated Delayed Fluorescent Emitters Featuring an Aggregation-Induced Emission Property. J Phys Chem Lett 2018;9(7):1547-53.
8. Leng P, Sun S, Guo R, Zhang Q, Liu W, Lv X, et al. Modifying the AIE-TADF chromophore with host-substituents to achieve high efficiency and low roll-off non-doped OLEDs. Org Electron. 2020;78:105602.
9. Koziar JC, Cowan DO. Photochemical heavy-atom effects. Acc Chem Res. 1978;11(9):334-41.
10. Gan S, Hu S, Li XL, Zeng J, Zhang D, Huang T, et al. Heavy Atom Effect of Bromine Significantly Enhances Exciton Utilization of Delayed Fluorescence Luminogens. ACS Appl Mater Interfaces. 2018;10(20):17327-34.
11. de Sa Pereira D, Lee DR, Kukhta NA, Lee KH, Kim CL, Batsanov AS, et al. The effect of a heavy atom on the radiative pathways of an emitter with dual conformation, thermally-activated delayed fluorescence and room temperature phosphorescence. J Mater Chem C. 2019;7(34):10481-90.
12. Xiang Y, Zhao Y, Xu N, Gong S, Ni F, Wu K, et al. Halogen-induced internal heavy-atom effect shortening the emissive lifetime and improving the fluorescence efficiency of thermally activated delayed fluorescence emitters. J Mater Chem C. 2017;5(46):12204-10.
13. Aizawa N, Harabuchi Y, Maeda S, Pu Y-J. Kinetic prediction of reverse intersystem crossing in organic donor–acceptor molecules. Nature Communications. 2020;11(1):3909.
14. Xu J, Zhu X, Guo J, Fan J, Zeng J, Chen S, et al. Aggregation-Induced Delayed Fluorescence Luminogens with Accelerated Reverse Intersystem Crossing for High-Performance OLEDs. ACS Materials Letters. 2019;1(6):613-9.

15. Matsuo K, Yasuda T. Blue thermally activated delayed fluorescence emitters incorporating acridan analogues with heavy group 14 elements for high-efficiency doped and non-doped OLEDs. Chem Sci. 2019;10(46):10687-97.
16. Kretzschmar A, Patze C, Schwaebel ST, Bunz UH. Development of Thermally Activated Delayed Fluorescence Materials with Shortened Emissive Lifetimes. J Org Chem. 2015;80(18):9126-31.
17. Kim CL, Jeong J, Lee DR, Jang HJ, Kim ST, Baik MH, et al. Dual Mode Radiative Transition from a Phenoselenazine Derivative and Electrical Switching of the Emission Mechanism. J Phys Chem Lett. 2020;11(14):5591-600.
18. Hall D, Suresh SM, dos Santos PL, Duda E, Bagnich S, Pershin A, et al. Improving Processability and Efficiency of Resonant TADF Emitters: A Design Strategy. Adv Optical Mater. 2019(n/a):1901627.
19. Hua T, Zhan L, Li N, Huang Z, Cao X, Xiao Z, et al. Heavy-Atom Effect Promotes Multi-Resonance Thermally Activated Delayed Fluorescence. ChemRxiv. 2021:DOI: 10.26434/chemrxiv.14046296.v1.
20. Pershin A, Hall D, Lemaur V, Sancho-Garcia JC, Muccioli L, Zysman-Colman E, et al. Highly emissive excitons with reduced exchange energy in thermally activated delayed fluorescent molecules. Nat Commun. 2019;10(1):597.
21. Zysman-Colman E, Arias K, Siegel JS. Synthesis of Arylbromides from Arenes and NBS in Acetonitrile: A Convenient method for Aromatic Bromination. Can J Chem. 2009;87(2):440-7.
22. Yan C, Shang R, Nakamoto M, Yamamoto Y, Adachi Y. The Substituent Effect of Bridged Triarylamine Helicenes on Light-emitting and Charge Transfer Properties. Chem Lett. 2020;49(5):457-60.